Laboratory Investigation (2012) 92, 1738–1748

Salvianolic acid B lowers portal pressure in cirrhotic rats and attenuates contraction of rat hepatic stellate cells by inhibiting RhoA signaling pathway

Hong Xu[1], Yang Zhou[1,2], Chao Lu[1], Jian Ping[1,2] and Lie-Ming Xu[1,2,3]

The contraction of hepatic stellate cells (HSCs) has a critical role in the regulation of intrahepatic vascular resistance and portal hypertension. Previous studies have confirmed that salvianolic acid B (Sal B) is effective against liver fibrosis. In the present study, we evaluated the effect of Sal B on portal hypertension and on HSCs contractility. Liver cirrhosis was induced in rats by peritoneal injection of dimethylnitrosamine and the portal pressure was measured. HSCs contraction was evaluated by collagen gel contraction assay. Glycerol-urea gel electrophoresis was performed to determine the phosphorylation of myosin light chain 2 (MLC2). F-actin stress fiber polymerization was detected by fluorescein isothiocyanate-labeled phalloidin. Intracellular Ca^{2+} and RhoA signaling activation were also measured. Sal B effectively reduced the portal pressure in DMN-induced cirrhotic rats. It decreased the contraction by endothelin-1 (ET-1)-activated HSCs by ~66.5% and caused the disassembly of actin stress fibers and MLC2 dephosphorylation. Although Sal B reduced ET-1-induced intracellular Ca^{2+} increase, blocking Ca^{2+} increase completely by BAPTA-AM, a Ca^{2+} chelator, barely affected the magnitude of contraction. Sal B decreased ET-1-induced RhoA and Rho-associated coiled coil-forming protein kinase (ROCK) II activation by 66.84% and by 76.79%, respectively, and inhibited Thr^{696} phosphorylation of MYPT1 by 80.09%. *In vivo*, Sal B lowers the portal pressure in rats with DMN-induced cirrhosis. *In vitro*, Sal B attenuates ET-1-induced HSCs contraction by inhibiting the activation of RhoA and ROCK II and the downstream MYPT1 phosphorylation at Thr^{696}. We consider Sal B a potential candidate for the pharmacological treatment of portal hypertension.
Laboratory Investigation (2012) **92,** 1738–1748; doi:10.1038/labinvest.2012.113; published online 17 September 2012

KEYWORDS: contraction; endothelin-1; hepatic stellate cells; RhoA/ROCK signaling pathway; salvianolic acid B

The role and regulation of contraction by hepatic stellate cells (HSCs) have been areas of active interest and investigation. These cells residing in the perisinusoidal space of Disse, serve as a major storage of vitamin A in normal liver. During chronic hepatic injury, HSCs undergo a process of transdifferentiation toward a myofibroblast phenotype. They consequently acquire enhanced contractility in response to a number of mediators, including endothelin-1 (ET-1), thrombin, angiotensin II and substance P. Among these, ET-1 is the most potent with abundant expression of ET receptors on HSCs.[1–3] HSCs regulate intrahepatic vascular resistance by contracting around sinusoid and are regarded as the potential therapeutic targets for the treatment of portal hypertension and liver fibrosis.[1,4,5]

Considerable efforts have been made to elucidate the signaling mechanisms regulating HSCs contraction. Ca^{2+}/MLCK pathway and RhoA/Rho-associated coiled coil-forming protein kinase (ROCK) pathway are two major and best-studied signaling pathways.[6,7] Ca^{2+} binds to calmodulin to activate myosin light chain kinase (MLCK), which phosphorylates myosin light chain 2 (MLC2). Moreover, the small G-protein RhoA activates its downstream effector ROCK, which in turn phosphorylates and thereby inactivates myosin light chain phosphatase (MLCP), leading to increased phosphorylation of MLC2.[8] The contractile apparatus is formed together by actin and myosin filaments. MLC2 phosphorylation triggers the activation of actomyosin ATPase, cross-bridge cycling and the subsequent force development. The opposing activities

[1]Institute of Liver Diseases, Shuguang Hospital Affiliated to Shanghai University of Traditional Chinese Medicine, Shanghai, China; [2]Key Laboratory of Liver and Kidney Diseases (Shanghai University of Traditional Chinese Medicine), Ministry of Education, Shanghai, China and [3]E-Institute of TCM Internal Medicine, Shanghai Municipal Education Commission, Shanghai, China
Correspondence: Professor L-M Xu, MD, Institute of Liver Diseases, Shuguang Hospital Affiliated to Shanghai University of Traditional Chinese Medicine, 528 Zhangheng Road, Shanghai 201203, China.
E-mail: xulieming@shutcm.edu.cn

Received 25 February 2012; revised 12 June 2012; accepted 14 June 2012

of MLCK and MLCP control the phosphorylation status of MLC2. Currently, the contribution of Ca^{2+} signaling for HSCs contraction has been largely challenged, while RhoA/ROCK pathway is considered as the primary signal transduction pathway that govern the force generation.[9]

An ideal drug to treat portal hypertension should be potent to decrease HSCs contractility. Current innovative strategies include delivering ROCK inhibitor Y-27632 directly to HSCs by coupling Y-27632 to carriers.[10] However, this strategy is in experimental development and is not applicable in a clinical setting. Previous studies have also indicated several pharmacological agents that can induce cytoskeleton disassembly and inhibit HSCs to contract.[11,12] Salvianolic acid B (Sal B) is one of the major water-soluble compounds of Salvia miltiorrhiza, which is widely used in China for the treatment of cardiovascular diseases.[13] Sal B is a potent antioxidant that has significant scavenging effects on oxygen free radicals, protecting against ischemia-reperfusion injuries in the heart and brain.[14] *In vitro*, it protects hepatocytes from CCl_4-induced cell damage, through inhibiting lipid peroxidation and eliminating ROS accumulation.[15] Available data also indicated that Sal B is effective against liver fibrosis.[16] However, there have been no reports on the effects of Sal B on portal hypertension. The present study indicates that apart from the antifibrotic effect, Sal B effectively reduces the elevated portal pressure in cirrhotic rats. Moreover, our data show for the first time that Sal B as a natural herb extract effectively reduces HSCs contraction.

MATERIALS AND METHODS

Materials

ET-1, collagenase type IV and fluorescein isothiocyanate (FITC)-labeled phalloidin were obtained from Sigma-Aldrich. Pronase E was from Roche Molecular Biochemicals and Nycodenz powder from Axis-Shield. ML-7 and Y-27632 were purchased from Calbiochem. Fluo4-AM and BAPTA-AM were from Invitrogen. Sal B (purity $>98\%$) was provided by Shanghai Medical Research Institute, Chinese Academy of Science. Rabbit anti-Thr^{696}-MYPT1, rabbit anti-Thr^{850}-MYPT1, recombinant MYPT1(654-880) and RhoA activation assay kit were from Upstate Biotechnology. Rabbit anti-MLC2, mouse anti-Ser^{19}-MLC2 and rabbit anti-ROCK I antibodies were obtained from Cell Signaling Technology. Mouse anti-ROCK II was a BD Bioscience product.

Animals

Male Sprague-Dawley rats (180–200 g) were initially randomized into two groups: control ($n=14$) and DMN group ($n=31$). The rats in DMN group were injected with DMN (10 mg/kg body weight) intraperitoneally for three consecutive days each week. At the end of the second week, two rats were killed for the fibrosis development assessment. The remaining DMN rats were further randomized into two groups: DMN model group ($n=13$) and Sal B group ($n=16$). Both groups continued to receive weekly DMN treatment for another 2 weeks in addition to daily administration of either water or Sal B, which were given intragastrically at a dose of 12.5 mg/kg body weight.

Histological Analysis

Liver tissues were fixed in 4% paraformaldehyde and dehydrated in a graded alcohol series. After embedded in paraffin, the tissues were sectioned at 5 μm in thickness and stained with hematoxylin–eosin or sirius red.

Portal Pressure Determination

Portal pressure was measured as described previously.[17] Laparotomy was performed and a PE tube (23 G) was inserted into the ileocolic vein and advanced to the confluence of the portal vein and splenic vein. This cannula was used to monitor portal pressure by a transducer system.

HSCs Isolation

HSCs were isolated from male Sprague-Dawley rats, weighing 400 to 500 g, as described previously.[18] In brief, following sequential *in situ* liver perfusion with pronase E and collagenase type IV, the resulting cell suspension was fractionated by density gradient centrifugation using Nycodenz solution. Cells were harvested at densities <1.065 g/ml and cultured in DMEM containing 10% fetal bovine serum. Experiments were performed on cells between first and third serial passages using three cultures from independent isolations.

Collagen Gel Contraction assay

Type I collagen was extracted by 0.1% acetic acid solution from rat tail tendons for collagen lattice preparation.[19] A mixture solution containing 1.2 mg/ml of collagen was poured into a 12-well plate and incubated for 1 h at 37 °C to allow gelation. Cells were layered on top of the formed lattices and grown to 90% confluence. After pretreatment with Sal B or/and inhibitors at certain concentrations for 30 min, cells were exposed to 10^{-8} M ET-1. The gels were immediately detached from the walls. Digital photos were obtained at 12-h intervals to monitor the change in lattice area.

Determination of MLC2 Phosphorylation

Control and treated monolayers were processed as described previously.[20] Proteins dissolved in urea sample buffer (20 mM Tris base, 22 mM glycine, 10 mM DTT, 8 M deionized urea and 0.1% bromphenol blue) were separated in glycerol gels (10% acrylamide, 40% glycerol, 20 mM Tris base and 22 mM glycine) and transferred to nitrocellulose membranes. The blots were probed with rabbit anti-MLC2 antibody or mouse anti-Ser^{19}-MLC2 phosphospecific antibody, followed by IRDye 680-conjugated goat anti-rabbit IgG or IRDye 800 CW donkey anti-mouse IgG. The blots were analyzed by Odyssey Infrared Imaging System. The extent of MLC2 phosphorylation was calculated as mol PO_4/mol MLC2 according the following formula: mol PO_4/mol

MLC2 = (monoP + 2 (diP))/(nonP + monoP + diP), where nonphosphorylated (nonP), monophosphorylated (monoP) and diphosphorylated (diP) represent the nonP, monoP and diP MLC2, respectively.

F-actin Staining

HSCs grown on glass coverslips were treated with ML-7 (10^{-5} M), Y-27632 (10^{-5} M) or Sal B (10^{-5} M) for 30 min, followed by incubation in media with or without ET-1 (10^{-8} M) for 30 min. After fixation with 3.7% paraformaldehyde, polymerized actin was stained by FITC-labeled phalloidin (5 μg/ml). Images were observed and captured by Olympus fluorescence microscopy.

Fluo-4 Visualization of Intracellular Ca^{2+}

Cells seeded on optical quality glass-bottomed 35-mm dishes were loaded with 5 μM Fluo4/0.04% PluronicF-127 in HBS for 45 min at 37 °C. Cells were then stimulated with ET-1(10^{-8} M) in 1.8 mM Ca^{2+} condition, with or without Sal B or BAPTA pretreatment for 30 min. Fluo-4 fluorescence was excited using a Kr/Ar laser at 488 nm and emitted fluorescence at 515 nm was collected.[9]

MYPT1 Phosphorylation

Equal amounts of cell lysates (50 µg) were loaded on 8% SDS-polyacrylamide gel, separated and transferred to nitrocellulose membranes. The blots were probed with rabbit anti-Thr^{696}-MYPT1 or rabbit anti-Thr^{850}-MYPT1, followed by horseradish peroxidase-conjugated anti-rabbit IgG. Signals were visualized by enhanced chemiluminescence detection.

RhoA Activation Assay

The activity of RhoA was determined by RhoA activation assay kit following the manufacturer's instructions.[21] Five-hundred micrograms of cell lysates were incubated with 30 μg of glutathione *S*-transferase (GST)-RBD (fusion protein containing the RhoA-binding domain of Rhotekin) complexed with agarose beads for 2 h at 4 °C with gentle agitation. Bound RhoA was eluted from the beads by boiling each sample in Laemmli reducing buffer. Eluted samples from the beads and total cell lysate were then electrophoresed on 12% SDS-polyacrylamide gel, followed by western blotting using mouse anti-RhoA monoclonal antibody.

ROCK Activation Assay

Five-hundred micrograms of lysates were prepared and immunoprecipitated as described previously by ROCK I or ROCK II monospecific antibody.[22] The beads were suspended in kinase assay buffer (20 mM MOPS, pH 7.2, 25 mM B-glycerophosphate, 5 mM EGTA, 15 mM $MgCl_2$ and 1 mM DTT) containing 10 μM ATP and 1 μg recombinant MYPT1(654-880), in a total reaction volume of 50 μl. Phosphorylated MYPT1(654-880) were detected by western blotting using anti-Thr^{696}-MYPT1 antibody.

Statistical Analysis

Data are presented as mean ± s.e.m. Statistical analysis of the results was performed using paired and unpaired Student's *t*-test as appropriate. $P < 0.05$ was considered statistically significant.

RESULTS

Sal B Reduces the Portal Pressure in DMN-Induced Cirrhotic Rats

Six rats died during the experiment, leaving 14 rats in control group (0 death), 9 rats in DMN model group (4 deaths) and 14 rats in Sal B group (2 deaths). In DMN model group, all rats had developed cirrhosis and portal hypertension, and six of nine rats had developed acites. Sal B decreased serum concentrations of ALT, AST and bilirubin, and hepatic hydroxyproline content (Figure1a). Hematoxylin–eosin and sirius red staining indicates significant fibrous septa, cirrhotic nodules and collagen deposition in the liver with cirrhosis. The lesions were largely alleviated by Sal B treatment (Figures 1b and c). The portal pressure was 5.9 ± 1.0 mm Hg in control, 13.9 ± 2.3 mm Hg in DMN model group and 9.2 ± 1.0 mm Hg in Sal B group (Figure 1d). The data indicate that Sal B treatment significantly reduces the portal hypertension in DMN-induced cirrhotic rats. Moreover, Sal B barely affects the heart rate in normal rats, and slightly increases the carotid artery pressure without showing any statistical significance (Figure 1e).

Sal B Inhibits ET-1-Induced HSCs Contraction

The purity of isolated rat HSCs was always higher than 95% as assessed by detecting vitamin A auto fluorescence and by characterization of typical retinoid droplets. Figure 2a shows the time-dependent activation of HSCs in culture. The contraction was evaluated using a model in which subcultured cells were grown on top of gel lattices composed of type-1 collagen. The lattice shrinkage in ET-1-treated cells was much stronger than in normal cells, with area 37.10 ± 5.10% *versus* 76.89 ± 3.84%. Pretreatment with 10^{-5} M ML-7 or 10^{-5} M Y-27632 significantly reduced the capability of HSCs to contract. The areas were 67.01 ± 4.14% and 77.28 ± 2.00%, respectively. 10^{-5} M Sal B led to ~66.5% of the contractile activity disappearence, showing an area of 63.58 ± 3.21%. As 10^{-2} M ML-7 stock solution was prepared in dimethylsulfoxide (DMSO), we added a control of 0.1% DMSO that barely affected the lattice shrinkage (Figures 2b and c).

Sal B Decreases ET-1-Induced MLC2 Phosphorylation

To investigate the phosphorylation status of MLC2, we performed glycerol-urea gel electrophoresis. In glycerol gels, different forms of MLC2 exhibit different migration rates that are diP > monoP > nonP MLC2. The extent of MLC2 phosphorylation was calculated as mol PO_4/mol MLC2. As shown in Figures 2d–g, untreated cells exhibited a basal

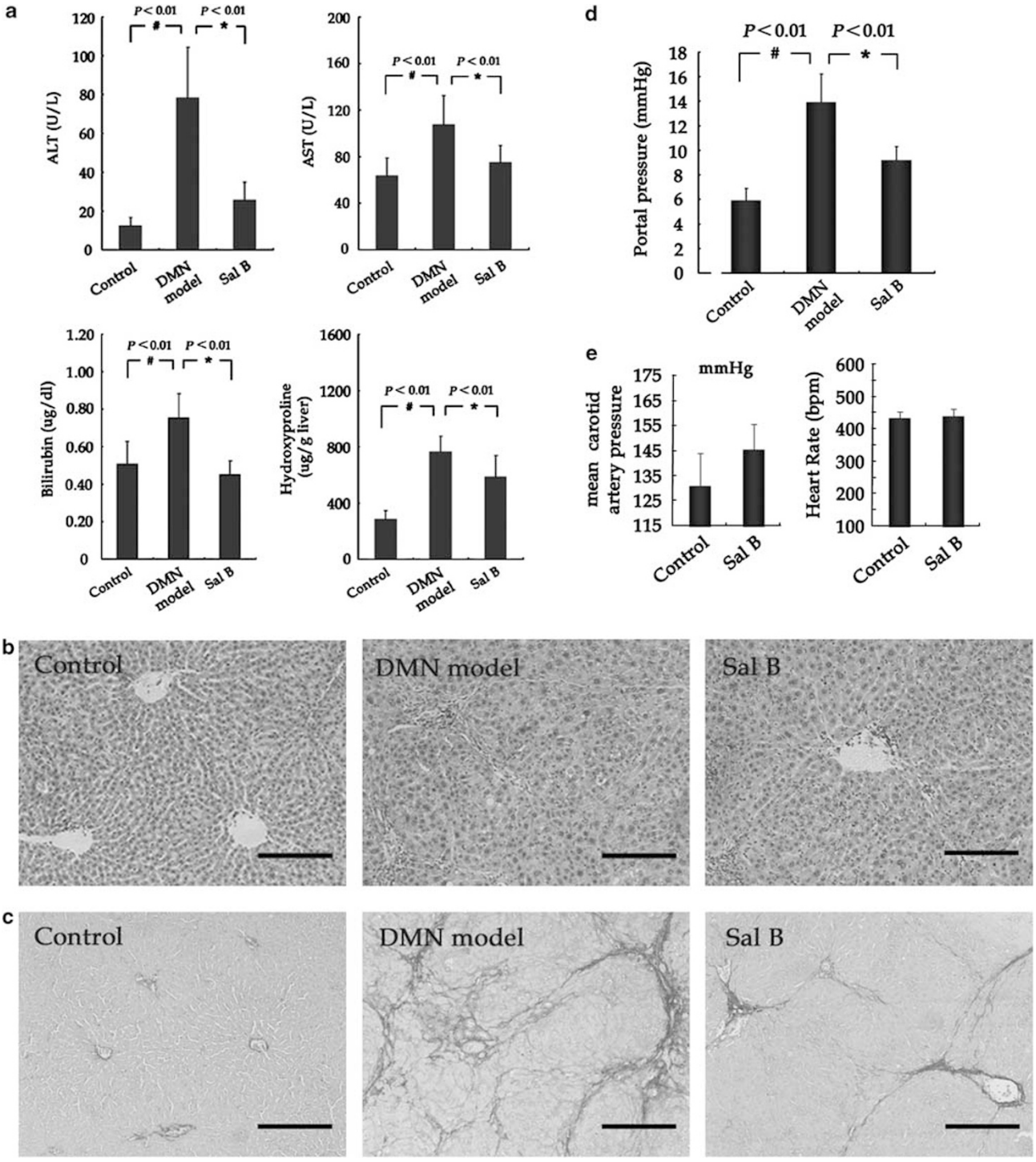

Figure 1 Sal B reduces the portal pressure and alleviates liver injury in DMN-induced cirrhotic rats. (**a**) Serum concentrations of ALT, AST and bilirubin and hepatic hydroxyproline content in control ($n=14$), DMN model ($n=9$) and Sal B-treated rats ($n=14$). (**b**–**c**) Hematoxylin–eosin and sirius red staining. Scale bar, 100 μm. (**d**) The portal pressure in control ($n=14$), DMN model ($n=9$) and Sal B-treated rats ($n=14$). #$P<0.01$ *versus* control, *$P<0.01$ *versus* DMN model group. (**e**) Treatment of Sal B for 2 weeks has no significant effect on either the carotid artery pressure or heart rate in normal rats (control $n=9$, Sal B $n=9$).

MLC2 phosphorylation of 0.35 ± 0.05 mol PO_4/mol MLC2. ET-1 elicited a rapid and sustained increase in both the content of mono- and diphosphorylated MLC2. The phosphorylation was 0.87 ± 0.04 mol PO_4/mol MLC2 by 5 min after ET-1 stimulation, and reached a maximal level of 0.96 ± 0.04 mol PO_4/mol MLC2 within 30 min. 10^{-5}M Y-27632 pretreatment completely suppressed MLC2 phosphorylation. Pretreatment by 10^{-5}M ML-7 and 10^{-5}M

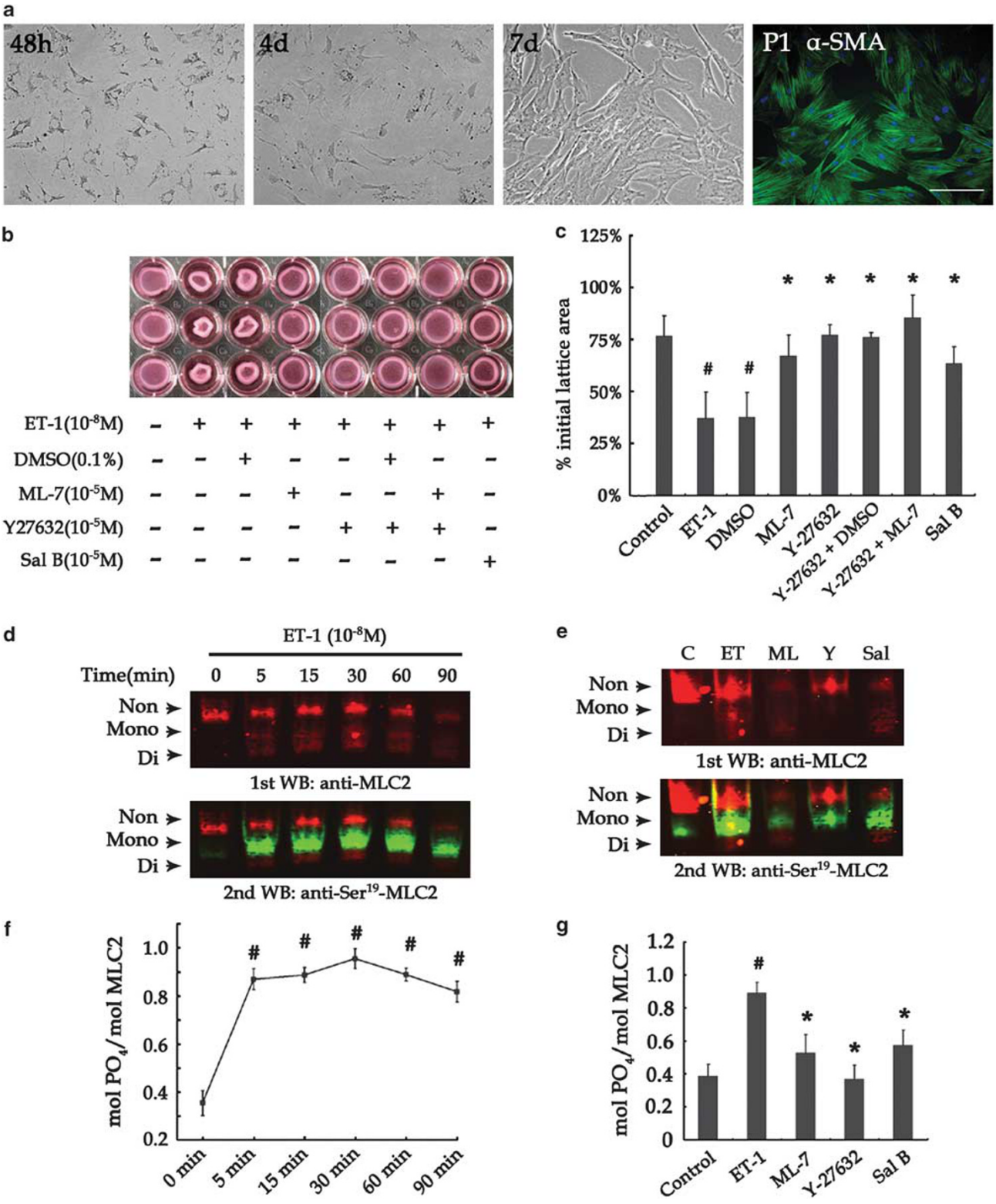

Figure 2 Sal B inhibits collagen lattice contraction by HSCs and decreases ET-1-induced MLC2 phosphorylation. (**a**) Time-dependent activation of rat HSCs in culture. Activated cells express α-SMA. Scale bar, 100 μm. (**b**) Appearance of collagen lattice at 48 h after dislodgement. (**c**) Graphic presentation shows the extent of contraction. Each experimental condition was carried out in triplicate and at least three independent experiments were performed. #$P<0.01$ *versus* control, *$P<0.01$ *versus* ET-1. (**d**–**e**) Cells were stimulated with ET-1 (10^{-8} M) for various time periods, or pretreated with ML-7 (10^{-5} M), Y-27632 (10^{-5} M) or Sal B (10^{-5} M) for 30 min before ET-1 stimulation. The nonP-, monoP- and diP-MLC2 were separated on 10% glycerol gel and the identity of these bands was verified using anti-Ser^{19}-MLC2 antibody (green). (**f**–**g**) The extent of MLC2 phosphorylation is calculated as mol PO_4/mol MLC2. Data from three independent experiments, #$P<0.01$ *versus* control, *$P<0.01$ *versus* ET-1.

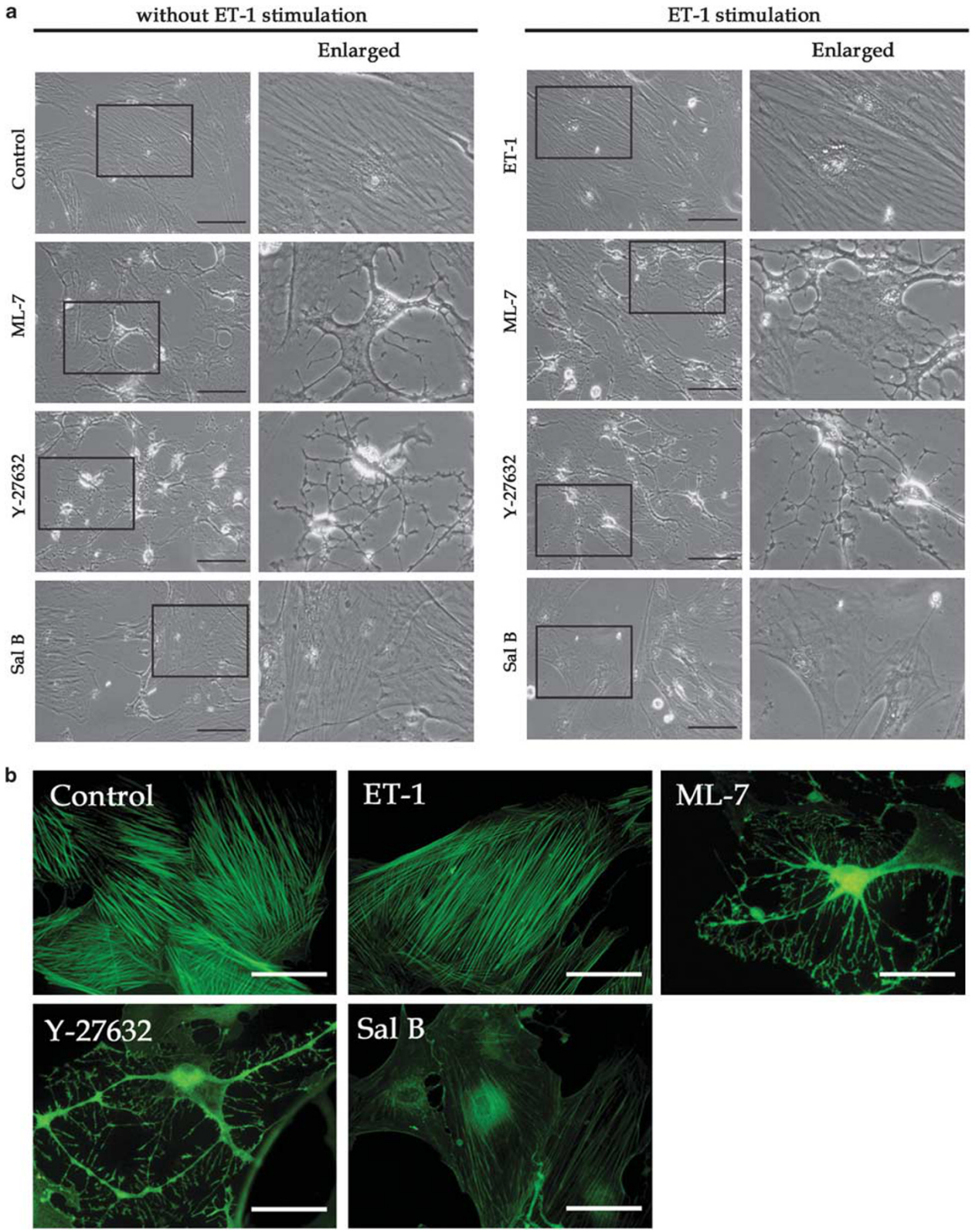

Figure 3 Sal B induces disassembly of actin stress fibers. (**a**) Cells were treated with ML-7 (10^{-5}M), Y-27632 (10^{-5}M) or Sal B (10^{-5}M) for 30 min, followed by incubation in media with or without ET-1 (10^{-8}M) for 30 min. Morphological change of cells was observed by phase-contrast microscopy. Enlarged views of the boxed areas are presented as indicated. Scale bar, 100 μm. (**b**) F-actin staining. Cells were pretreated with ML-7 (10^{-5}M), Y-27632 (10^{-5}M) or Sal B (10^{-5}M) for 30 min, then stimulated with ET-1 (10^{-8}M) for 30 min. F-actin was stained by FITC-labeled phalloidin. Scale bar, 100 μm.

Sal B decreased ET-1-induced phosphorylation by 71.9% and by 63.1%, respectively.

Sal B Induces the Disassembly of Actin Stress Fibers

Actin assembly is required for HSCs contractibility. As shown in Figure 3, control and ET-1-treated cells displayed a polygonal morphology with dense bundles of stress fibers aligning along the major axis of the cell. While treated with ML-7 or Y-27632, the actin polymerization was severely ablated with cells showing arborized appearance. The arborization effect was not reversed by ET-1 stimulation. Sal B also caused the disassembly of stress fibers with a few randomly dispersed actin filaments throughout the cytoplasm.

Sal B Reduces ET-1-Induced Ca^{2+} Increase and Inhibits RhoA Activation

We observed that ET-1 elicited an immediate influx in intracellular Ca^{2+} that peaked at 1 min and rapidly returned to basal level within 3 min. Pretreatment of Sal B partially reduced the Ca^{2+} increase induced by ET-1. The Ca^{2+} chelator BAPTA-AM, which was used as a positive control, completely blocked the increase in cytosolic Ca^{2+}. However,

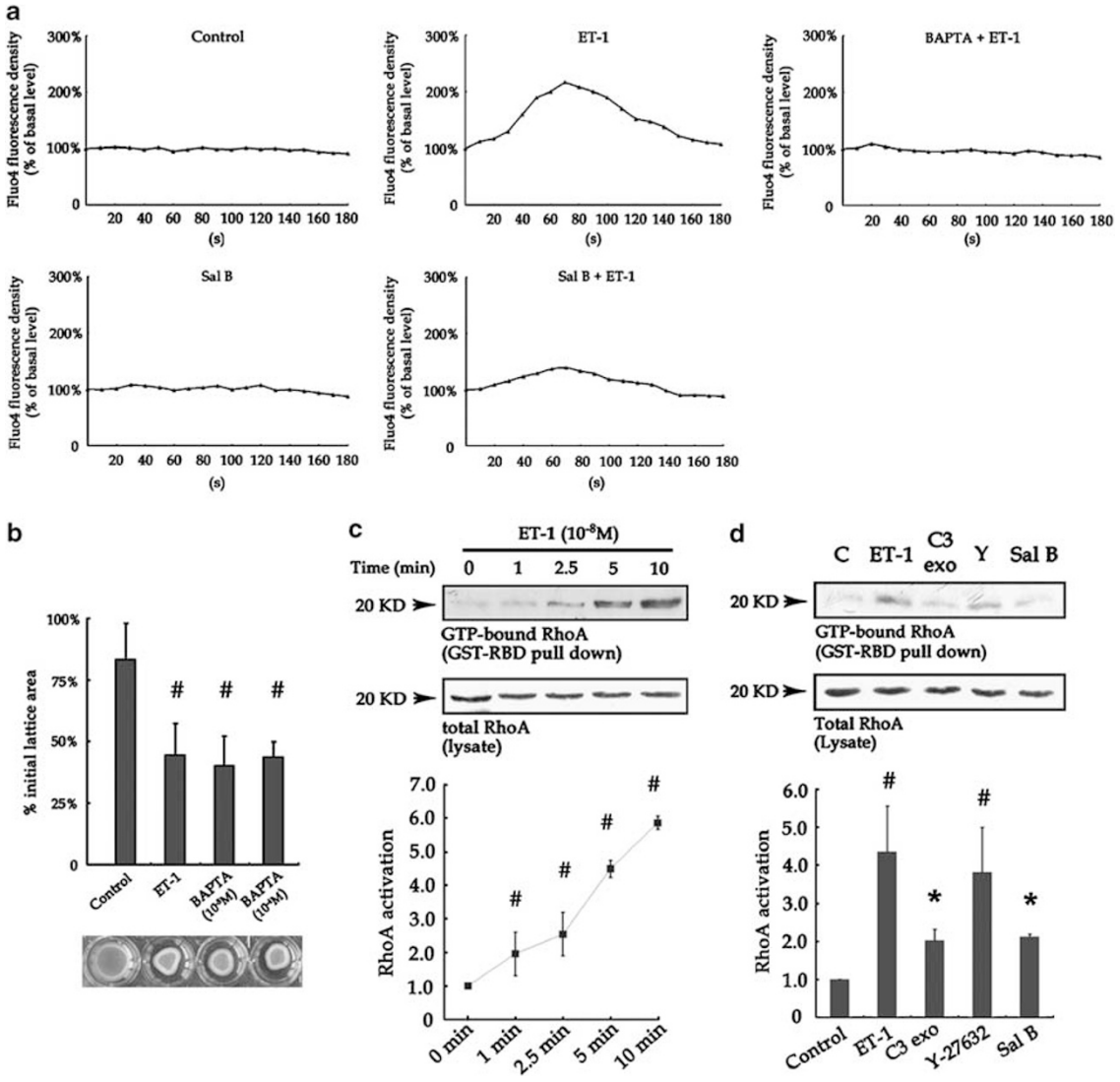

Figure 4 Sal B reduces ET-1-induced intracellular Ca^{2+} increase and inhibits RhoA activation. (**a**) Changes of Ca^{2+} were observed by Fluo-4 fluorescence. Cells loaded with Fluo4-AM were stimulated with ET-1(10^{-8}M) in 1.8 mM Ca^{2+} condition, with or without Sal B or BAPTA pretreatment for 30 min. Cells were visualized, and images were captured every 10 s. (**b**) BAPTA barely affected ET-1-induced HSCs contraction. (**c**) The activation course of RhoA upon ET-1 stimulation. (**d**) Cells were pretreated with Y-27632 (10^{-5}M) or Sal B (10^{-5}M) for 30 min, or with C3 exoenzyme (10 μg/ml) for 24 h before ET-1 incubation for 10 min. Activated (GTP-bound) RhoA was selectively pulled down by Rho-binding domain of Rhotekin coupled to agarose beads. RhoA activity is represented as the relative ratio of the density of GTP-RhoA against that of total RhoA. Data are representative of three independent experiments. #$P<0.01$ *versus* control, *$P<0.01$ *versus* ET-1.

BAPTA-AM barely affected the magnitude of contraction (Figures 4a and b).

We next evaluated whether Sal B has an inhibitory effect on RhoA signaling pathway. To determine the activity of RhoA, Rhotekin-binding assay was performed using RhoA-binding domain from Rhotekin, a downstream effector of RhoA. This fragment binds only GTP-bound active RhoA, but fails to react with GDP-bound RhoA. The activation was determined by comparing relative proportions of GTP-bound RhoA to total RhoA. ET-1 stimulation produced a time-dependent increase in RhoA activity by nearly 1.95-fold over control within 60 s and 5.84-fold at 10 min (Figure 4c). 10 μg/ml C3 exoenzyme, an ADP-ribose transferase and Sal B decreased ET-1-induced RhoA activation by 69.76% and 66.84%, respectively. The ROCK inhibitor Y-27632 had no significant effect on RhoA activity (Figure 4d).

Sal B Inhibits ET-1-Induced ROCK II Activation

ROCK I and ROCK II were detected simultaneously in rat HSCs with an identical molecular weight of 160 kDa (Figure 5a) and were immunoprecipitated by monospecific antibodies. Using recombinant MYPT1(654-880) as a substrate, *in vitro* phosphorylation assay was carried out to measure the catalytic activities of ROCKs. In untreated control cells, minimal activities of ROCK I and ROCK II were detectable as exhibited by a very low level of Thr^{696}-MYPT1(654-880). ET-1 treatment produced a time-dependent increase in ROCK II activity, achieving a maximal activation of 4.83-fold over control after 10 min (Figure 5c). ROCK I activity had no significant change upon ET-1 stimulation (Figure 5b). Y-27632 and Sal B pretreatment reduced ET-1-induced ROCK II activation by 99.55% and 76.79%, respectively (Figure 5d).

Sal B Inhibits MYPT1 Phosphorylation at Thr^{696}, but not at Thr^{850}

MLCP is a heterotrimeric protein composed of a 37-kDa catalytic subunit of type 1 protein phosphatase (PP-1c), a110–130-kDa regulatory myosin phosphatase targeting subunit (MYPT1) and a 20-kDa subunit of unknown function.[23] The activity of MLCP is mainly regulated by phosphorylation of the MYPT-1 subunit. Several phosphorylation sites have been identified on MYPT-1, including Thr^{696} (133-kDa isoform, human) and Thr^{850} (133-kDa isoform, chicken), that can be phosphorylated by ROCK.[24,25] We showed that MYPT1 from untreated control HSCs exhibited a basal level of phosphorylation at Thr^{696}. ET-1 stimulation increased Thr^{696} phosphorylation up to 3.86-fold over control within 2.5 min, reaching a maximal level of 5.17-fold by 15 min (Figure 6a). Basal phosphorylation was also detected at Thr^{850} in control cells. Peak Thr^{850} phosphorylation was observed by 15 min after ET-1 addition, reaching 3.3-fold compared with control (Figure 6b). Sal B pretreatment decreased ET-1-induced Thr^{696} phosphorylation by nearly 80.09%, while Y-27632 caused a more sharp decrease in Thr^{696} phosphorylation by 104.80% (Figure 6c). In contrast, pretreatment with Y-27632 or Sal B

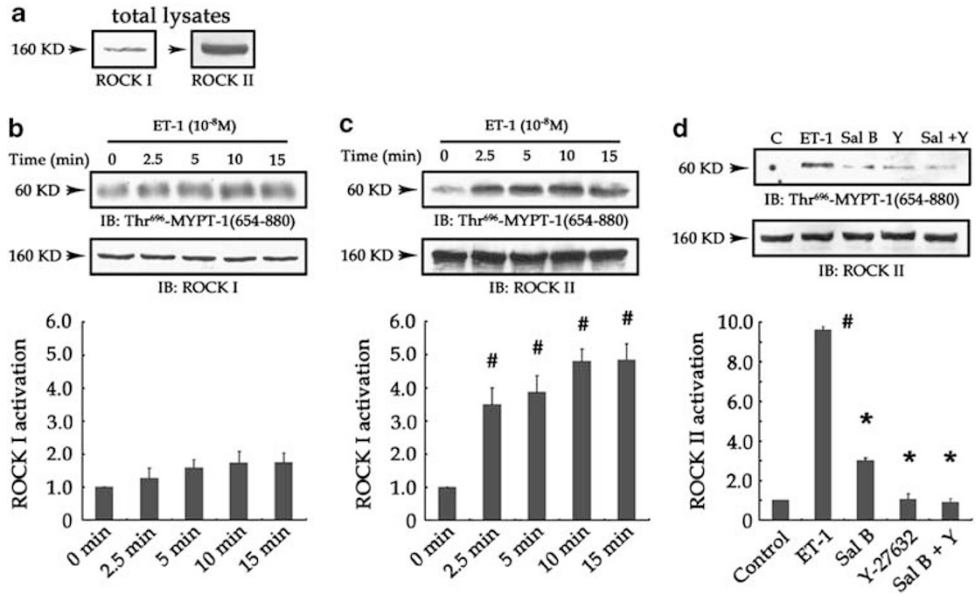

Figure 5 Sal B inhibits ET-1-induced ROCK II activation. (**a**) The expression of two isoforms of ROCK in rat HSCs. (**b**–**c**) ROCK I and ROCK II activation in response to ET-1 stimulation. Cells were treated with 10^{-8}M ET-1 for various time intervals. ROCK I and ROCK II were precipitated using monospecific antibodies and were used for *in vitro* phosphorylation reactions with recombinant MYPT1(654-880) as a substrate. Phosphorylated MYPT1(654-880) was analyzed on 8% SDS-PAGE and detected by anti-Thr^{696}-MYPT1 antibody. Immunoprecipitated ROCK I or ROCK II demonstrated the equal loading of proteins. (**d**) Cells were pretreated with 10^{-5}M Y-27632, 10^{-5}M Sal B, or with both for 30 min, then incubated with 10^{-8}M ET-1 for 15 min. The mean density of Thr^{696}-MYPT1(654-880) was normalized by that of ROCK II, and control samples were assigned a value of 1. Data are representative of three independent experiments. #$P<0.01$ *versus* control, *$P<0.01$ *versus* ET-1.

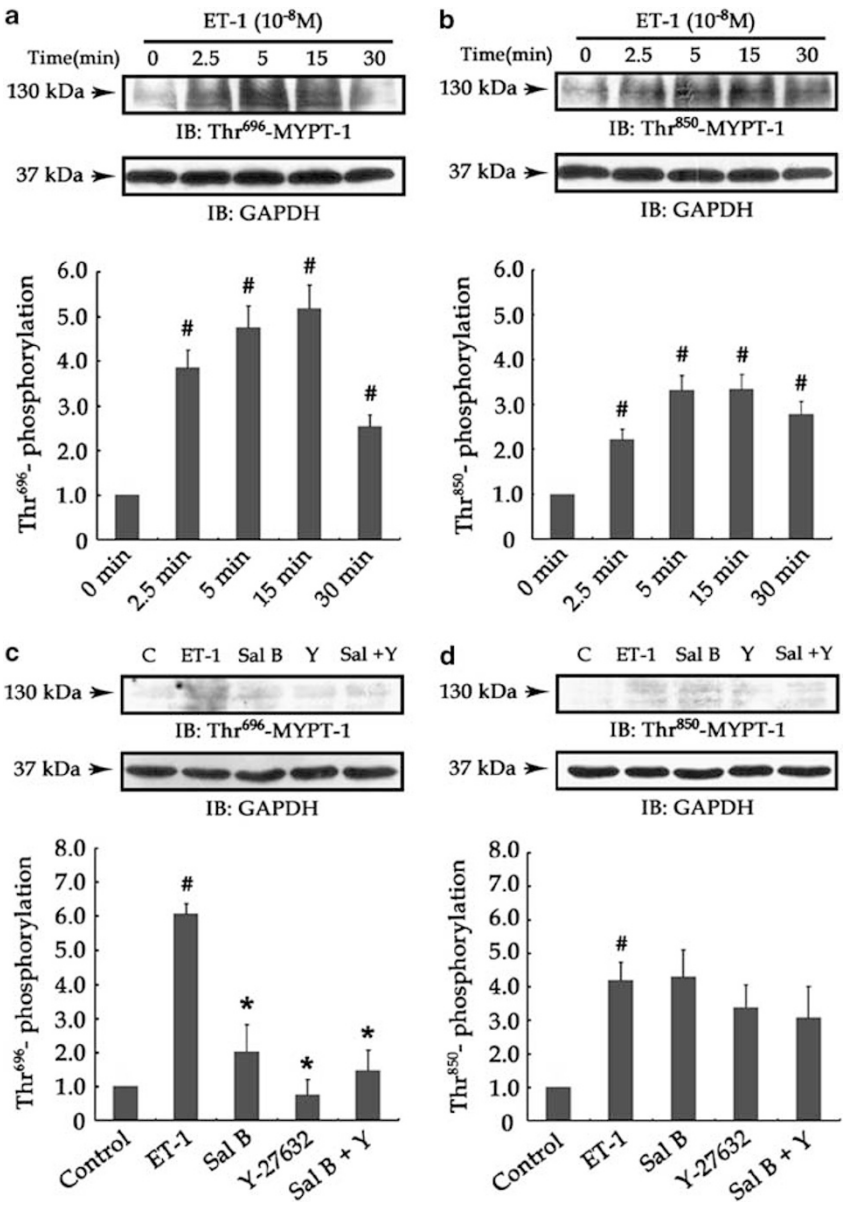

Figure 6 Sal B inhibits MYPT1 phosphorylation at Thr^{696}, but not Thr^{850}. (**a**–**b**) MYPT-1 phosphorylation at Thr^{696} and at Thr^{850} upon ET-1 stimulation. (**c**–**d**) Cells were pretreated with 10^{-5} M Sal B and 10^{-5} M Y-27632, alone or in combination for 30 min, then stimulated with 10^{-8} M ET-1 for 15 min. Cell lysates were separated on 8% SDS-PAGE followed by western blotting using anti-Thr^{696}-MYPT1 or anti-Thr^{850}-MYPT1 antibodies. The mean density of Thr^{696}- or Thr^{850}-MYPT1 was normalized by that of GAPDH and control samples were set at 1 arbitrary unit. Data from three independent experiments, #$P<0.01$ *versus* control, *$P<0.01$ *versus* ET-1.

did not cause a significant change in Thr^{850} phosphorylation (Figure 6d).

DISCUSSION

Our data have been expanded on previous work to demonstrate that Sal B, the most abundant component of Salvia miltiorrhiza, decreases the portal pressure in rats with DMN-induced cirrhosis. Furthermore, Sal B significantly reduces *in vitro* contraction of ET-1-activated HSCs and inhibits the activation of intracellular RhoA/ROCK II signaling pathway. This is for the first time indicating that Sal B acts directly on HSCs contractility through RhoA inhibition.

HSCs have a pivotal role in modulating intrahepatic vascular resistance by contracting around sinusoid. Apart from the increased HSCs contractility, structural changes such as fibrotic scar tissue and collagen deposition also contribute to increased intrahepatic resistance. Augmented portal blood flow, which results from hyperdynamic circulation in the splanchnic and systemic blood vessels, occurs in a more

advanced stage of portal hypertension.[1,5] Our results also show that Sal B is effective against fibrosis and reduces collagen deposition in the liver. Treatment with Sal B has no significant effects on either the carotid artery pressure or the heart rate. Thus, we consider that Sal B may not affect systemic hemodynamics. However, the possibility of Sal B's splanchnic effect could not be excluded. According to the present study, the decreased portal pressure by Sal B may be attributed to the decreased intrahepatic resistance, which is a consequence of alleviation of liver injury and fibrosis and decreased contraction of activated HSCs.

Understanding the signaling mechanisms by which Sal B regulates HSCs contractility is of considerable importance. We observed an immediate fluctuation of Ca^{2+} in the cytoplasm after ET-1 addition. Pretreatment of Sal B effectively reduced ET-1-stimulated Ca^{2+} increase. Thus, we speculate that Sal B inhibits HSCs contraction by suppression of Ca^{2+} signaling pathway. But blocking Ca^{2+} elevation completely by BAPTA-AM, a Ca^{2+} chelator, barely affected the magnitude of contraction. This result is consistent with previous study, which indicated that changes in cytosolic Ca^{2+} were neither necessary nor sufficient to provoke HSCs contraction.[9]

Our results also showed that Y-27632 and ML-7 significantly blocked the lattice shrinkage by ET-1-activated HSCs. The combined use of ML-7 and Y-27632 had a stronger effect than saturating concentrations of either inhibitor alone, suggesting that MLCK and ROCK have complementary effects on HSCs contraction. However, the apparent contradictory results obtained with ML-7 and BAPTA-AM could not be explained, as Ca^{2+} is thought to regulate contraction by activating MLCK. According to the literature, a proportion of MLCK activity may be mediated in a Ca^{2+}-independent way and would not be ablated by Ca^{2+}-free condition.[26] The Ca^{2+}-independent MLCK activity seems to be strong enough to provoke the force development. Whether there are signaling links between RhoA pathway and MLCK activation are not clear and remains to be further studied.

Sal B significantly decreased ET-1-induced activation of RhoA and downstream effector ROCK II. To date, the role of RhoA signaling in HSCs has been mostly learned by copying that in smooth muscles. Detailed information about the dynamic changes, isoforms or phosphorylation status of functional molecules in this signaling cascade in HSCs is incompletely understood. ROCK I and ROCK II, two isoforms of ROCK, are assumed to perform the same functions. They are highly homologous and phosphorylate the same substrates like MYPT1 or MLC2.[27] Moreover, Y-27632 and other commercially available ROCK inhibitors inhibit the activities of two isoforms with almost equal potency. Only rare studies have drawn distinctions between two isoforms.[28,29] The present study discloses that the activation of ROCK II is highly regulated while ROCK I activity barely changed upon ET-1 stimulation. They may not have equivalent roles during HSCs contraction.

Both Thr^{696} and Thr^{850} phosphorylation of MYPT1 have been detected in HSCs and increase in a time-dependent way in response to ET-1 stimulation. Thr^{696} phosphorylation increases more sharply than Thr^{850} phosphorylation. Of interest is that Sal B or Y-27632 pretreatment largely prevents MYPT1 phosphorylation at Thr^{696}, but has no effect on Thr^{850} phosphorylation. As Y-27632 is a specific ROCK inhibitor and almost completely inhibits HSCs contractility, we consider that: first, Thr^{696} rather than Thr^{850} is required for the regulation of MLCP activity and HSCs contraction. This is consistent with previous findings, in which Thr^{696}, but not Thr^{850}, has been identified as a crucial inhibitory site.[25] Second, Thr^{850} may be not an endogenous target of ROCK in HSCs and phosphorylation at this site is dominantly regulated by other kinases.

We consider Sal B an ideal drug to treat portal hypertension. Compared with other pharmacological agents,[11,12,30] Sal B not only decreases the portal pressure but also is antifibrotic and decreases the contraction of activated HSCs. The effect of Sal B on HSCs contractility is mainly attributed to the suppression of RhoA/ROCK II pathway, which results in the disassembly of actin stress fibers and MLC2 dephosphorylation. As we mentioned above, Sal B also inhibits the transient increase in cytosolic Ca^{2+}, suggesting that Sal B has a pleiotropic effect on both Ca^{2+} and RhoA signaling pathways. However, the precise molecular target of Sal B remains unclear. As Ca^{2+} and RhoA are located upstream of Ca^{2+} and RhoA signaling cascade, respectively, we speculate that Sal B may affect the interaction of ET-1 and ET-1 receptor. This speculation needs to be further clarified. Considering that BAPTA-AM barely affects the contractility of activated HSCs, we also hypothise that in HSCs, RhoA pathway is able to compensate for the complete blocking of Ca^{2+} to generate sufficient contractile force.

Collectively, our data provide evidence that Sal B lowers the portal pressure in rats with DMN-induced cirrhosis. Sal B also significantly reduces HSCs contractility by inhibiting RhoA/ROCK II activation and the downstream MYPT1 phosphorylation at Thr^{696}. We consider Sal B as a potential candidate for the pharmacological treatment of portal hypertension.

ACKNOWLEDGEMENTS

This work was supported by National Natural Science Foundation of China (30672489), Shanghai Leading Academic Discipline Project (Y0302), Leading Academic Discipline Project of Shanghai Municipal Education Commission (J50307) and E-Institute of TCM Internal Medicine (E03008).

DISCLOSURE/CONFLICT OF INTEREST

The authors declare no conflict of interest.

1. Reynaert H, Thompson MG, Thomas T, *et al*. Hepatic stellate cells: role in microcirculation and pathophysiology of portal hypertension. Gut 2002;50:571–581.
2. Rockey DC. Vascular mediators in the injured liver. Hepatology 2003;37:4–12.

3. Housset C, Rockey DC, Bissell DM. Endothelin receptors in rat liver: lipocytes as a contractile target for endothelin 1. Proc Natl Acad Sci USA 1993;90:9266–9270.
4. Thimgan MS, Yee Jr. HF. Quantitation of rat hepatic stellate cell contraction: stellate cells' contribution to sinusoidal resistance. Am J Physiol 1999;277(1 Pt 1):G137–G143.
5. Friedman SL. Hepatic stellate cells: protean, multifunctional, and enigmatic cells of the liver. Physiol Rev 2008;88:125–172.
6. Bataller R, Nicolás JM, Gineès P, *et al.* Contraction of human hepatic stellate cells activated in culture: a role for voltage-operated calcium channels. J Hepatol 1998;29:398–408.
7. Yee Jr HF. Ca^{2+} and rho signaling pathways: two paths to hepatic stellate cell contraction. Hepatology 2001;33:1007–1008.
8. Etienne-Manneville S, Hall A. Rho GTPases in cell biology. Nature 2002; 420:629–635.
9. Melton AC, Datta A, Yee Jr. HF. $[Ca^{2+}]_i$-independent contractile force generation by rat hepatic stellate cells in response to endothelin-1. Am J Physiol Gastrointest Liver Physiol 2006;290:G7–G13.
10. van Beuge MM, Prakash J, Lacombe M, *et al.* Reduction of fibrogenesis by selective delivery of a Rho kinase inhibitor to hepatic stellate cells in mice. J Pharmacol Exp Ther 2011;337:628–635.
11. Sohail MA, Hashmi AZ, Hakim W, *et al.* Adenosine induces loss of actin stress fibers and inhibits contraction in hepatic stellate cells via Rho inhibition. Hepatology 2009;49:185–194.
12. Liu Z, van Grunsven LA, Van Rossen E, *et al.* Blebbistatin inhibits contraction and accelerates migration in mouse hepatic stellate cells. Br J Pharmacol 2010;159:304–315.
13. Ho JH, Hong CY. Salvianolic acids: small compounds with multiple mechanisms for cardiovascular protection. J Biomed Sci 2011;18:30.
14. Chen YH, Du GH, Zhang JT. Salvianolic acid B protects brain against injuries caused by ischemia-reperfusion in rats. Acta Pharmacol Sin 2000;21:463–466.
15. Lin YL, Wu CH, Luo MH, *et al. In vitro* protective effects of salvianolic acid B on primary hepatocytes and hepatic stellate cells. J Ethnopharmacol 2006;105:215–222.
16. Tsai MK, Lin YL, Huang YT. Effects of salvianolic acids on oxidative stress and hepatic fibrosis in rats. Toxicol Appl Pharmacol 2010;242: 155–164.
17. Steib CJ, Hennenberg M, Beitinger F, *et al.* Amiloride reduces portal hypertension in rat liver cirrhosis. Gut 2010;59:827–836.
18. Cassiman D, Denef C, Desmet VJ, *et al.* Human and rat hepatic stellate cells express neurotrophins and neurotrophin receptors. Hepatology 2001;33:148–158.
19. Montesano R, Orci L. Transforming growth factor beta stimulates collagen-matrix contraction by fibroblasts: implications for wound healing. Proc Natl Acad Sci USA 1988;85:4894–4897.
20. Satpathy M, Gallagher P, Lizotte-Waniewski M, *et al.* Thrombin-induced phosphorylation of the regulatory light chain of myosin II in cultured bovine corneal endothelial cells. Exp Eye Res 2004;79: 477–486.
21. Emmert DA, Fee JA, Goeckeler ZM, *et al.* Rho-kinase-mediated Ca^{2+}-independent contraction in rat embryo fibroblasts. Am J Physiol Cell Physiol 2004;286:C8–C21.
22. Ling L, Lobie PE. RhoA/ROCK activation by growth hormone abrogates p300/histone deacetylase 6 repression of Stat5-mediated transcription. J Biol Chem 2004;279:32737–32750.
23. Ito M, Nakano T, Erdodi F, *et al.* Myosin phosphatase: structure, regulation and function. Mol Cell Biochem. 2004;259:197–209.
24. Kawano Y, Fukata Y, Oshiro N, *et al.* Phosphorylation of myosin-binding subunit (MBS) of myosin phosphatase by Rho-kinase *in vivo*. J Cell Biol 1999;147:1023–1038.
25. Feng J, Ito M, Ichikawa K, *et al.* Inhibitory phosphorylation site for Rho-associated kinase on smooth muscle myosin phosphatase. J Biol Chem 1999;274:37385–37390.
26. Saitoh M, Ishikawa T, Matsushima S, *et al.* Selective inhibition of catalytic activity of smooth muscle myosin light chain kinase. J Biol Chem 1987;262:7796–7801.
27. Nakagawa O, Fujisawa K, Ishizaki T, *et al.* ROCK-I and ROCK-II, two isoforms of Rho-associated coiled-coil forming protein serine/ threonine kinase in mice. FEBS Lett 1996;392:189–193.
28. Thumkeo D, Keel J, Ishizaki T, *et al.* Targeted disruption of the mouse rho-associated kinase 2 gene results in intrauterine growth retardation and fetal death. Mol Cell Biol 2003;23:5043–5055.
29. Yoneda A, Ushakov D, Multhaupt HA, *et al.* Fibronectin matrix assembly requires distinct contributions from Rho kinases I and -II Mol Biol Cell 2007;18:66–75.
30. Trebicka J, Hennenberg M, Laleman W, *et al.* Atorvastatin lowers portal pressure in cirrhotic rats by inhibition of RhoA/Rho-kinase and activation of endothelial nitric oxide synthase. Hepatology 2007;46: 242–253.